SIAM J. SCI. COMPUT.
Vol. 23, No. 6, pp. 2075–2095

CHEBYSHEV SPECTRAL METHODS FOR RADIATIVE TRANSFER*

ARNOLD D. KIM† AND MIGUEL MOSCOSO‡

Abstract. We study the performance of Chebyshev spectral methods for time-dependent radiative transfer equations. Starting with a method for one-dimensional problems in homogeneous media, we show that the modifications needed to consider more general problems such as inhomogeneous media, polarization, and higher dimensions are straightforward. In this method, we approximate the spatial dependence of the intensity by an expansion of Chebyshev polynomials. This yields a coupled system of integro-differential equations for the expansion coefficients that depend on angle and time. Next, we approximate the integral operation on the angle variables using a Gaussian quadrature rule resulting in a coupled system of differential equations with respect to time. Using a second-order finite difference approximation, we discretize the time variable. We solve the resultant system of equations with an efficient algorithm that makes Chebyshev spectral methods competitive with other methods for radiative transfer equations.

Key words. Chebyshev spectral method, radiative transfer

AMS subject classifications. 65M70, 35Q60, 78A45, 78A48

PII. S1064827500382312

1. Introduction.

Spectral methods have been widely applied to the Navier–Stokes [1, 2], Schrödinger [3], acoustic [4], and Maxwell [5] equations, among others, with great success. In this paper we are interested in using a Chebyshev spectral method [6, 7] for the vector radiative transfer equation

$$\frac{1}{v}\frac{\partial}{\partial t}\mathbf{I}(\mathbf{r},\widehat{\Omega},t)+\widehat{\Omega}\cdot\nabla_{\mathbf{r}}\mathbf{I}(\mathbf{r},\widehat{\Omega},t)+\mathcal{Q}[\mathbf{I}](\mathbf{r},\widehat{\Omega},t)=\mathbf{F}(\mathbf{r},\widehat{\Omega},t) \tag{1.1}$$

governing wave propagation in a medium $\mathcal{D}\subset\mathbb{R}^n$ $(n=1,2,3)$ that scatters, absorbs, depolarizes, and emits radiation. Applications for the vector radiative transfer equation include polarized light propagation in clouds, fog, rain, and biological tissue [8] as well as seismic wave propagation in heterogeneous media [10, 11]. In (1.1) $\mathbf{I}=(I,Q,U,V)$ is the 4×1 Stokes vector needed to describe the polarized radiation field completely. The total intensity is represented by I, the linear polarization state by Q and U, and the circular polarization state by V. The Stokes vector $\mathbf{I}$ depends on position $\mathbf{r}\in\mathbb{R}^n$, direction $\widehat{\Omega}\in\mathbb{S}^2$ ($\mathbb{S}^2$ denotes the surface of the unit sphere), and time $t\in[0,T]$. In (1.1), v is the constant wave speed in the medium, and

$$\mathcal{Q}[\mathbf{I}](\mathbf{r},\widehat{\Omega},t)=\sigma_t(\mathbf{r})\mathbf{I}(\mathbf{r},\widehat{\Omega},t)-\sigma_s(\mathbf{r})\int_{\mathbb{S}^2}\mathbf{S}(\widehat{\Omega},\widehat{\Omega}')\,\mathbf{I}(\mathbf{r},\widehat{\Omega}',t)\,d\widehat{\Omega}' \tag{1.2}$$

is the scattering operator. The total scattering cross-section $\sigma_t(\mathbf{r})$ is the sum of the scattering cross-section $\sigma_s(\mathbf{r})$ and the absorption cross-section $\sigma_a(\mathbf{r})$. All of these cross-sections are real and nonnegative. The scattering matrix $\mathbf{S}(\widehat{\Omega},\widehat{\Omega}')$, which we

*Received by the editors December 8, 2000; accepted for publication (in revised form) November 15, 2001; published electronically February 27, 2002.
http://www.siam.org/journals/sisc/23-6/38231.html

†Department of Mathematics, 450 Serra Mall, Building 380, Stanford University, Stanford, CA 94305-2125 (adkim@math.stanford.edu). This author's research was supported by NSF grant DMS-0071578.

‡Departamento de Matemáticas, Escuela Politécnica Superior, Universidad Carlos III de Madrid, Avda. de la Universidad 30, 28911 Leganés, Spain (mmoscoso@math.stanford.edu). This author's research was supported by AFOSR grant 49620-98-1-0211 and by NSF grant 9709320.

assume is position independent, describes the directional distribution of energy density that scatters in direction $\widehat{\Omega}$ due to unit energy density incident in direction $\widehat{\Omega}'$. In addition, this matrix describes polarization changes manifested by scattering. Finally, the source term $\mathbf{F}(\mathbf{r}, \widehat{\Omega}, t)$ accounts for any sources contained in the medium.

The radiative transfer equation has to be solved with appropriate initial and boundary conditions. We assume that no radiation other than the source $\mathbf{F}$ enters into the medium so that

$$\mathbf{I}(\mathbf{r}, \widehat{\Omega}, t) = 0 \quad \text{on} \quad \Gamma, \tag{1.3}$$

where $\Gamma = \{(\mathbf{r}, \widehat{\Omega}, t) \in \partial\mathcal{D} \times \mathbb{S}^2 \times [0, T] \text{ such that } \nu(\mathbf{r}) \cdot \widehat{\Omega} < 0\}$, and $\nu(\mathbf{r})$ denotes the unit outward normal vector to the boundary $\partial\mathcal{D}$. In addition, we assume that no energy is present in the medium at time $t = 0$,

$$\mathbf{I}(\mathbf{r}, \widehat{\Omega}, 0) = 0 \quad \text{in} \quad \mathcal{D} \times \mathbb{S}^2. \tag{1.4}$$

The transport problem (1.1)–(1.4) is well-posed [12]. It models the incoherent or scattered intensity for which its source manifests from coherent intensity incident at the boundary [8, 9].

Equation (1.1) is usually solved using Monte Carlo methods (see [13] and references therein for details). The main advantage of Monte Carlo methods is their relative simplicity and their ability to handle complicated geometries. For large optical depths, they require a large number of particles to obtain statistical accuracy leading to long computational times. Other common numerical methods such as finite differences and finite elements have been applied to the scalar radiative transfer equation with no polarization. However, for vector problems, Monte Carlo methods are preferred.

Despite the high accuracy and competitive cost of spectral methods, there is not, to our knowledge, any attempt to solve the time-dependent, vector radiative transfer equation using spectral methods. However, there are two works that are related to this problem. Ritchie, Dykema, and Braddy [14] solve the scalar, time-dependent problem radiative transfer equation in which polarization is neglected with a Fourier spectral method. Kim and Ishimaru [15] solve the one-dimensional, time-independent, vector radiative transfer equation in homogeneous media with Chebyshev spectral methods. In contrast to Fourier methods, which are restricted to problems with periodic boundary conditions, Chebyshev spectral methods can consider a broad variety of boundary conditions [7]. This is important for many applications such as optical imaging [16].

In this paper, we show that the underlying ideas of the Chebyshev spectral method shown in [15] are robust to generalizations such as time-dependent, inhomogeneous, and higher-dimensional problems. Keeping the ease of implementation and the low computational cost of a basic algorithm, we introduce modifications needed for these general problems. In section 2, we start with the basic algorithm for the one-dimensional, scalar problem in homogeneous media. We generalize this method to inhomogeneous, vector, and higher-dimensional problems in section 3. We present results from numerical experiments in section 4. A summary of our work and some concluding remarks appear in section 5.

2. Time-dependent, scalar problems in one-dimensional homogeneous media. In this section, let us consider the plane-parallel problem shown in Figure 2.1. The medium, which infinitely extends in the x-y directions, is bounded by two planes located at $z = 0$ and $z = d$, and its spatial properties, σ_t and σ_s, are constant.

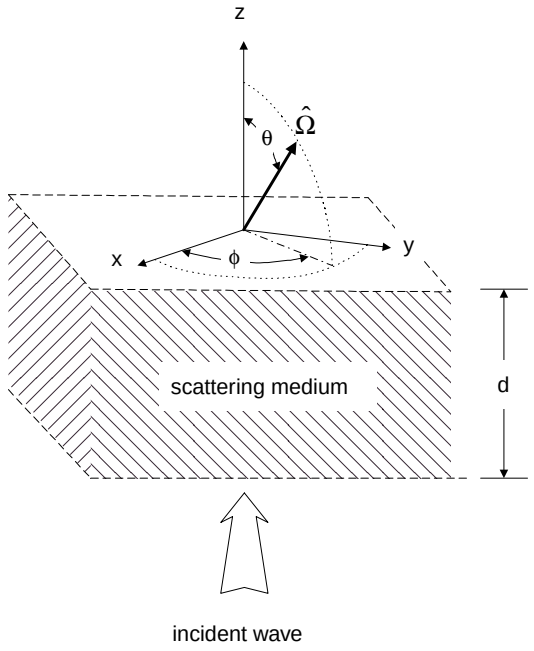

Fig. 2.1. *The plane-parallel problem.*

In addition, the source F does not vary with respect to x and y. We also neglect polarization so that $Q = U = V = 0$ in (1.1)–(1.4), and the 4×4 matrix $\mathbf{S}(\widehat{\Omega} \cdot \widehat{\Omega}')$ is replaced by the scalar function $P(\widehat{\Omega}, \widehat{\Omega}') = \mathbf{S}_{11}(\widehat{\Omega}, \widehat{\Omega}')$ (the $(1,1)$ entry of $\mathbf{S}$). The scalar function P is called the phase function. Under these assumptions, the vector radiative transport equation (1.1) reduces to

$$\frac{1}{v}\frac{\partial}{\partial t} I(z,\mu,\phi,t) + \mu \frac{\partial}{\partial z} I(z,\mu,\phi,t) + \mathcal{Q}[I](z,\mu,\phi,t) = F(z,\mu,\phi,t), \tag{2.1}$$

with

$$\mathcal{Q}[I] = \sigma_t I(z,\mu,\phi,t) - \sigma_s \int_0^{2\pi} \int_{-1}^{1} P(\mu,\mu',\phi-\phi')\, I(z,\mu',\phi',t)\, d\mu' d\phi'. \tag{2.2}$$

Here, $\mu = \cos\theta$, where θ is the propagation direction angle defined with respect to the positive z-direction, and ϕ is the azimuthal angle (see Figure 2.1). The special form of the azimuthal dependence, $\phi - \phi'$, in the phase function P is a direct consequence of the rotational invariance of the scattering matrix.

By representing the azimuthal dependence of the intensity as a Fourier series,

$$I(z,\mu,\phi,t) = \sum_{n=-\infty}^{\infty} I_n(z,\mu,t)\, \mathrm{e}^{in\phi}, \tag{2.3}$$

where the coefficients of this expansion are defined as

$$I_n(z,\mu,t) = \frac{1}{2\pi} \int_0^{2\pi} I(z,\mu,\phi,t)\, \mathrm{e}^{-in\phi} d\phi, \tag{2.4}$$

one finds that each Fourier mode decouples from the others in (2.1). Dropping the index n for simplicity, we find that the resultant problem for each harmonic is

$$\frac{1}{v}\frac{\partial}{\partial t}I(z,\mu,t)+\mu\frac{\partial}{\partial z}I(z,\mu,t)+\mathcal{Q}[I](z,\mu,t)=F(z,\mu,t) \quad \text{in} \quad \mathbb{X}, \tag{2.5a}$$

$$I(z=0,\mu,t)=0 \quad \text{on} \quad (0,1]\times[0,T], \tag{2.5b}$$

$$I(z=d,\mu,t)=0 \quad \text{on} \quad [-1,0)\times[0,T], \tag{2.5c}$$

$$I(z,\mu,t=0)=0 \quad \text{in} \quad [0,d]\times[-1,1], \tag{2.5d}$$

where $\mathbb{X}=[0,d]\times[-1,1]\times[0,T]$ and

$$\mathcal{Q}[I]=\sigma_t I(z,\mu,t)-\sigma_s\int_{-1}^{1}p(\mu,\mu')\,I(z,\mu',t)\,d\mu'. \tag{2.6}$$

In (2.5a) F is a coefficient of an azimuthal Fourier series expansion of the source. Here, we distinguish the Fourier coefficient of the phase function P defined in (1.2) by p in (2.6). It is normalized according to

$$\int_{-1}^{1}p(\mu,\mu')d\mu'=1.$$

Henceforth, we concentrate on solving (2.5) for only one Fourier mode since each mode is decoupled from the others.

2.1. Spatial discretization. Let us change variables in (2.5) from $z\in[0,d]$ to $s\in[-1,1]$ by the linear transformation $s=2z/d-1$. Under this change of variables, (2.5a) becomes

$$\frac{1}{v}\frac{\partial}{\partial t}I(s,\mu,t)+\frac{2}{d}\mu\frac{\partial}{\partial s}I(s,\mu,t)+\mathcal{Q}[I](s,\mu,t)=F(s,\mu,t). \tag{2.7}$$

Now we approximate the spatial dependence of the intensity by the Chebyshev spectral expansion

$$I(s,\mu,t)\cong\sum_{k=0}^{N}a_k(\mu,t)T_k(s). \tag{2.8}$$

The Chebyshev polynomials $T_k(s)$ are orthogonal with respect to the weighted inner product

$$(T_j,T_k)=\int_{-1}^{1}T_j(s)\,T_k(s)\,\frac{ds}{\sqrt{1-s^2}}=\begin{cases}\pi\delta_{j,k} & \text{for } k=0,\\ \frac{\pi}{2}\delta_{j,k} & \text{for } k\geq 1\end{cases} \tag{2.9}$$

and are normalized so that $T_k(s=\pm1)=(\pm1)^k$. Here, $\delta_{j,k}$ is the Kronecker delta. Since the expansion functions T_k do not satisfy the boundary conditions (2.5b) and (2.5c), the extra set of equations

$$I(s=-1,\mu,t)=\sum_{k=0}^{N}(-1)^k a_k(\mu,t)=0 \qquad \text{on } (0,1]\times[0,T], \tag{2.10a}$$

$$I(s=+1,\mu,t)=\sum_{k=0}^{N}a_k(\mu,t)=0 \qquad \text{on } [-1,0)\times[0,T] \tag{2.10b}$$

must be included. Each boundary condition imposes the value of the intensity only over half of the angular data ($\mu < 0$ or $\mu > 0$). Therefore, the composition of (2.10a) and (2.10b) defines a single equation for the expansion coefficients on $[-1, 1] \times [0, T]$. Furthermore, we note that considering different boundary conditions does not alter any other aspect of this method.

The Chebyshev spectral approximation to (2.7) is given by (2.8) with (2.10) and

$$\frac{1}{v}\frac{\partial a_k}{\partial t} + \frac{2}{d}\mu\left(T_k, \frac{\partial I}{\partial s}\right) + (T_k, \mathcal{Q}[I]) = (T_k, F), \qquad k = 0, \ldots, N. \tag{2.11}$$

Next, we approximate the spatial derivative by another spectral expansion,

$$\frac{\partial I(s, \mu, t)}{\partial s} \cong \sum_{k=0}^{N} A_k(\mu, t) T_k(s), \tag{2.12}$$

where A_k is related to a_k through

$$a_k = \frac{1}{2k}\left[c_{k-1}A_{k-1} - A_{k+1}\right] \quad \text{for } k = 1, 2, \ldots, N. \tag{2.13}$$

In (2.13), we assume that $A_{N+1} \ll A_N$ so that $a_N = \frac{1}{2N}c_{N-1}A_{N-1}$. The normalization quantity c_k is defined as

$$c_k = \begin{cases} 2 & \text{for } k = 0, \\ 1 & \text{for } k = 1, \ldots, N-1. \end{cases} \tag{2.14}$$

Substituting (2.8) and (2.12) into (2.11) we obtain the system of integro-differential equations

$$\frac{\partial a_k(\mu, t)}{\partial t} + \frac{2v}{d}\mu A_k(\mu, t) + v\mathcal{Q}[a_k](\mu, t) = vF_k(\mu, t), \qquad k = 0, \ldots, N, \tag{2.15}$$

for the expansion coefficients a_k and A_k. Note that there are $N+1$ equations in (2.15), an extra equation due to the boundary condition (2.10), plus the N relations (2.13) for the $2N+2$ unknowns in $\{a_k, A_k\}$. Later in this discussion, we use (2.13) to reduce the number of unknowns to $N+1$. In (2.15), F_k are the coefficients of the Chebyshev spectral approximation of the source function. Finally, we note that the resolution requirements needed to compute an accurate numerical solution of the system do not directly depend on the thickness of the medium $z = d$. Rather, spectrally resolving the source function over the spatial domain dictates the resolution requirements. In other words, sources that rapidly vary in the spatial domain require more Chebyshev modes than smoothly varying ones.

2.1.1. Angular discretization. In using a Chebyshev spectral approximation for the spatial variable, we obtain the integro-differential system (2.15) for expansion coefficients that depend on angle and time. We now focus attention on accurately treating the scattering operation. While there are several different ways of treating the integral operation in the radiative transfer equation, such as spherical harmonics and finite element expansions, a simple and effective method is the discrete ordinate method. By using this method, one can accurately approximate the scattering operator and easily adjust the angular resolution needed for different levels of anisotropy. Methods using spherical harmonics expansions require moderately

low levels of anisotropy for efficient use. Otherwise, the number of spherical harmonics needed becomes restrictively large for practical computations. Finite element methods are useful for highly anisotropic scattering [20] but are more complicated to implement than discrete ordinate methods. Choosing any of these methods for the angular discretization would work without interfering with the rest of the algorithm.

Now let us replace the continuous angular variable μ with a set of discrete points $\{\mu_i\}$. Then

$$\frac{\partial a_k(\mu_i,t)}{\partial t}+\frac{2v}{d}\mu_i A_k(\mu_i,t)+v\mathrm{Q}[a_k](\mu_i,t)=vF_k(\mu_i,t)\qquad\text{for } i=1,\dots,q, \tag{2.16}$$

where $k=0,\dots,N$. We use these discrete points μ_i to approximate the scattering operator as

$$\mathrm{Q}[a_k](\mu_i,t)=\sigma_t a_k(\mu_i,t)-\sigma_s\sum_{j=1}^{q}w_j p(\mu_i,\mu_j)\,a_k(\mu_j,t). \tag{2.17}$$

The quality of this approximation will of course depend on the choice of the quadrature rule. We refer to [17] and references therein for a more detailed discussion on this subject. We chose a quadrature rule where μ_j are the zeros of the Legendre polynomial of order q and w_j are the corresponding Gaussian weights.

Using matrix notation, (2.16) can be written as

$$\frac{\partial \mathbf{a}_k(t)}{\partial t}+\frac{2v}{d}\mathrm{L}\mathbf{A}_k(t)+v\mathrm{Q}[\mathbf{a}_k](t)=v\mathbf{F}_k(t)\qquad\text{for } k=0,\dots,N, \tag{2.18}$$

where we have introduced the $q\times 1$ vectors

$$\mathbf{a}_k(t)=(a_k(\mu_1,t),a_k(\mu_2,t),\dots,a_k(\mu_q,t)), \tag{2.19a}$$

$$\mathbf{A}_k(t)=(A_k(\mu_1,t),A_k(\mu_2,t),\dots,A_k(\mu_q,t)), \tag{2.19b}$$

$$\mathbf{F}_k(t)=(F_k(\mu_1,t),F_k(\mu_2,t),\dots,F_k(\mu_q,t)), \tag{2.19c}$$

and the $q\times q$ matrix $\mathrm{L}=\mathrm{diag}(\mu_1,\mu_2,\dots,\mu_q)$.

2.2. Temporal discretization. To integrate (2.18) in time, we use a trapezoid rule and obtain

$$\left[\mathbb{I}+\frac{v\Delta t}{2}\mathrm{Q}\right]\mathbf{a}_k^{n+1}+\frac{v\Delta t}{d}\mathrm{L}\mathbf{A}_k^{n+1}=\left[\mathbb{I}-\frac{v\Delta t}{2}\mathrm{Q}\right]\mathbf{a}_k^{n}-\frac{v\Delta t}{d}\mathrm{L}\mathbf{A}_k^{n}+\frac{v\Delta t}{2}\left[\mathbf{F}_k^{n+1}+\mathbf{F}_k^{n}\right], \tag{2.20}$$

where $\mathbb{I}$ is the identity matrix and $\mathbf{a}_k^n$ and $\mathbf{A}_k^n$ are the coefficients for the intensity and its spatial derivative evaluated at time $t_n=n\Delta t$, respectively. The numerical scheme (2.20) corresponds to the Crank–Nicholson method which is fully implicit, second-order accurate, and unconditionally stable.

Now we discuss an efficient algorithm to solve (2.20). At each time step we must solve

$$\mathrm{K}\mathbf{a}_k+\mathrm{M}\mathbf{A}_k=\mathbf{f}_k, \tag{2.21}$$

where $\mathrm{K}=\mathbb{I}+v\Delta t\mathrm{Q}/2$, $\mathrm{M}=v\Delta t\mathrm{L}/d$, and $\mathbf{f}_k$ is a known quantity corresponding to the right-hand side of (2.20).

From (2.13) we see that transforming from $\mathbf{a}_k$ to $\mathbf{A}_k$ is a simple operation possessing an inherent sparsity. To take advantage of this sparsity, we construct a system of equations to solve for the coefficients of the intensity's spatial derivative rather than coefficients of the intensity (see [18] and references therein for details regarding this technique). After transforming terms involving $\mathbf{a}_k$ to operations on $\mathbf{A}_k$, we obtain a block tridiagonal system

$$\mathrm{M}\mathbf{A}_0 + \mathrm{K}\mathbf{a}_0 = \mathbf{f}_0 \qquad \text{for } k = 0, \tag{2.22a}$$

$$\mathrm{M}\mathbf{A}_1 + \mathrm{K}\mathbf{A}_0 - \frac{1}{2}\mathrm{K}\mathbf{A}_2 = \mathbf{f}_1 \qquad \text{for } k = 1, \tag{2.22b}$$

$$\mathrm{M}\mathbf{A}_k + \frac{1}{2k}\mathrm{K}\left[\mathbf{A}_{k-1} - \mathbf{A}_{k+1}\right] = \mathbf{f}_k \qquad \text{for } k = 2, \ldots, N-1, \tag{2.22c}$$

$$\mathrm{M}\mathbf{A}_N + \frac{1}{2N}\mathrm{K}\mathbf{A}_{N-1} = \mathbf{f}_N \qquad \text{for } k = N. \tag{2.22d}$$

For the boundary conditions (2.5b) and (2.5c), we evaluate each expansion coefficient a_k at the quadrature points μ_i and operate on that result by (2.13) to obtain

$$\mathbf{a}_0^+ - \mathbf{A}_0^+ + \frac{1}{4}\mathbf{A}_1^+ - \sum_{k=2}^{N-1} \frac{(-1)^k}{2}\left[\frac{1}{k+1} - \frac{1}{k-1}\right]\mathbf{A}_k^+ + \frac{1}{2(N-1)}\mathbf{A}_N^+ = 0, \tag{2.23a}$$

$$\mathbf{a}_0^- + \mathbf{A}_0^- + \frac{1}{4}\mathbf{A}_1^- + \sum_{k=2}^{N-1} \frac{1}{2}\left[\frac{1}{k+1} - \frac{1}{k-1}\right]\mathbf{A}_k^- - \frac{1}{2(N-1)}\mathbf{A}_N^- = 0. \tag{2.23b}$$

Here, we have defined $\mathbf{A}_k^{\mp}$ to be subvectors of $\mathbf{A}_k$,

$$\mathbf{A}_k = \begin{bmatrix} \mathbf{A}_k^- \\ \mathbf{A}_k^+ \end{bmatrix}, \tag{2.24}$$

where $\mathbf{A}_k^-$ corresponds to the part of $\mathbf{A}_k$ in which $\mu_i < 0$ and $\mathbf{A}_k^+$ corresponds to the part of $\mathbf{A}_k$ in which $\mu_i > 0$. The same notation applies for $\mathbf{a}_0^{\mp}$.

Equations (2.22) and (2.23) define a system of equations for $\mathbf{A}_0, \mathbf{A}_1, \ldots, \mathbf{A}_N$ and $\mathbf{a}_0$. After computing a solution for these unknowns, we can compute the desired expansion coefficients of the intensity $\mathbf{a}_k$ by applying (2.13) again. One can solve this system using Gaussian elimination, but the cost is $O\left(q^3(N+1)^3\right)$. Instead, we use the generalized deflated block elimination method [19] that takes advantage of the inherent sparsity of this system to reduce the number of operations significantly. The number of operations needed to solve (2.22) and (2.23) using this method is $O(q^3(N-1))$. We discuss the details of this solution method in Appendix A.

3. Generalizations. We now study the modifications needed to deal with more general problems. We carry out these modifications in a way that preserves the order of accuracy, computational cost, and ease of implementation.

3.1. Layered media. In many applications the properties of the medium in the vertical direction are not homogeneous. In that case, a multilayered model where the scattering and total cross-sections are piecewise constant functions in space might be applied. Using the Chebyshev spectral method, we find that solving problems in layered media is essentially the same as solving homogeneous problems in each

layer. Dealing with interfaces between layers requires only adding extra conditions that reside with the boundary conditions in the resultant system of equations.

For simplicity, let us consider a medium with only two layers. In that case

$$\sigma_{s,t}(z) = \begin{cases} \sigma_{s,t}^{(1)} & \text{for } z \in [0, d_1), \\ \sigma_{s,t}^{(2)} & \text{for } z \in [d_1, d_2]. \end{cases} \tag{3.1}$$

In addition to the boundary conditions (2.5b) and (2.5c), we impose that the intensity at the interface $z = d_1$ between the layers is continuous so that

$$I(z, \mu, t) = \begin{cases} I^{(1)}(z, \mu, t) & \text{for } z \in [0, d_1], \\ I^{(2)}(z, \mu, t) & \text{for } z \in [d_1, d_2]. \end{cases} \tag{3.2}$$

Now let us introduce two spatial variables

$$s_1 = 2\frac{z}{d_1} - 1 \qquad \text{for } z \in [0, d_1], \tag{3.3}$$

$$s_2 = 2\frac{z - d_1}{d_2 - d_1} - 1 \quad \text{for } z \in [d_1, d_2] \tag{3.4}$$

so that the radiative transfer equation for each harmonic is

$$\left[\frac{1}{v}\frac{\partial}{\partial t} + \frac{2}{d_1}\mu\frac{\partial}{\partial s_1} + \mathcal{Q}^{(1)}\right] I^{(1)}(s_1, \mu, t) = F^{(1)}(s_1, \mu, t) \qquad \text{for } s_1 \in [-1, 1], \tag{3.5a}$$

$$\left[\frac{1}{v}\frac{\partial}{\partial t} + \frac{2}{d_2 - d_1}\mu\frac{\partial}{\partial s_2} + \mathcal{Q}^{(2)}\right] I^{(2)}(s_2, \mu, t) = F^{(2)}(s_2, \mu, t) \quad \text{for } s_2 \in [-1, 1]. \tag{3.5b}$$

Here, we define the scattering operator as

$$\mathcal{Q}^{(j)}[I] = \sigma_t^{(j)} I(s_j, \mu, t) - \sigma_s^{(j)} \int_{-1}^{1} p(\mu, \mu') I(s_j, \mu', t)\, d\mu', \qquad j = 1, 2, \tag{3.6}$$

and the source function as

$$F(z, \mu, t) = \begin{cases} F^{(1)}(z, \mu, t) & \text{for } z \in [0, d_1], \\ F^{(2)}(z, \mu, t) & \text{for } z \in [d_1, d_2]. \end{cases} \tag{3.7}$$

The boundary conditions for this problem are

$$I^{(1)}(s_1 = -1, \mu, t) = 0 \qquad \text{on} \quad (0, 1] \times [0, T], \tag{3.8a}$$

$$I^{(2)}(s_2 = +1, \mu, t) = 0 \qquad \text{on} \quad [-1, 0) \times [0, T], \tag{3.8b}$$

and the continuity condition at the interface implies that

$$I^{(1)}(s_1 = +1, \mu, t) = I^{(2)}(s_2 = -1, \mu, t) \qquad \text{on} \quad [-1, 1] \times [0, T]. \tag{3.9}$$

Now we consider Chebyshev spectral approximations for $I^{(1)}$ and $I^{(2)}$:

$$I^{(j)}(s_j, \mu, t) \cong \sum_{k=0}^{N} a_k^{(j)}(\mu, t) T_k(s_j), \qquad j = 1, 2. \tag{3.10}$$

In performing the same analysis used for the homogeneous case, we obtain

$$\frac{\partial}{\partial t}a_k^{(1)}(\mu,t) + \frac{2v}{d_1}\mu A_k^{(1)}(\mu,t) + v\mathcal{Q}^{(1)}[a_k^{(1)}](\mu,t) = vF_k^{(1)}(\mu,t), \tag{3.11a}$$

$$\frac{\partial}{\partial t}a_k^{(2)}(\mu,t) + \frac{2v}{d_2-d_1}\mu A_k^{(2)}(\mu,t) + v\mathcal{Q}^{(2)}[a_k^{(2)}](\mu,t) = vF_k^{(2)}(\mu,t) \tag{3.11b}$$

for $k = 0$ u 4 Γ + 4 Tfi 2 z 6] (7 h - + W c b b b c 4 Γ 4 z 4 Tfh z + fi z F 4 - 8 + F 8 W F

We first express the variable cross-sections as

$$\sigma_{s,t} = \sigma_{s,t}^{(0)} + \tilde{\sigma}_{s,t}(s), \tag{3.14}$$

where $\sigma_s^{(0)}$ and $\sigma_t^{(0)}$ are constants. We choose to represent the variable cross-sections in this way so we can treat a portion of the cross-section implicitly. This is important for the time stability limit of the scheme. By substituting (3.14) into the radiative transfer equation, we obtain

$$\frac{1}{v}\frac{\partial}{\partial t}I(s,\mu,t) + \frac{2}{d}\mu\frac{\partial}{\partial s}I(s,\mu,t) + \mathcal{Q}[I](s,\mu,t) = F(s,\mu,t) - \tilde{\mathcal{Q}}[I](s,\mu,t), \tag{3.15}$$

with

$$\tilde{\mathcal{Q}}[I](s,\mu,t) = \tilde{\sigma}_t(s)I(s,\mu,t) - \tilde{\sigma}_s(s)\int_{-1}^{1} p(\mu,\mu')\, I(s,\mu',t)\, d\mu'. \tag{3.16}$$

The only difference between (2.7) for the homogeneous case and (3.15) is the inhomogeneous term $\tilde{\mathcal{Q}}[I]$.

In order to maintain high accuracy and low computational cost, we treat $\tilde{\mathcal{Q}}[I]$ explicitly in time with a second-order Adams–Bashforth scheme so that

$$\begin{aligned}\left[\mathbb{I} + \frac{v\Delta t}{2}\mathrm{Q}\right]\mathbf{a}_k^{n+1} + \frac{v\Delta t}{d}\mathrm{L}\mathbf{A}_k^{n+1} = \left[\mathbb{I} - \frac{v\Delta t}{2}\mathrm{Q}\right]\mathbf{a}_k^{n} - \frac{v\Delta t}{d}\mathrm{L}\mathbf{A}_k^{n} \\ + \frac{v\Delta t}{2}\left[\mathbf{F}_k^{n+1} + \mathbf{F}_k^{n}\right] - \frac{v\Delta t}{2}\left[3\tilde{\mathrm{Q}}[\mathbf{a}]_k^n - \tilde{\mathrm{Q}}[\mathbf{a}]_k^{n-1}\right].\end{aligned} \tag{3.17}$$

The convolution terms

$$[\tilde{\sigma}_{t,s} \star a]_k^n(\mu_i) = \int_{-1}^{1} \tilde{\sigma}_{t,s}(s)I(s,\mu_i,t_n)T_k(s)\frac{ds}{\sqrt{1-s^2}} \tag{3.18}$$

contained within $\tilde{\mathrm{Q}}[\mathbf{a}]_k^n$ are evaluated explicitly in time, so there is no coupling between different k modes at time level $n+1$. These convolutions can be computed either in the spatial domain (pseudospectrally) or in the Chebyshev transform domain. Notice that the only difference between the homogeneous and inhomogeneous problem lies in constructing the right-hand side of (3.17).

Dealing with the inhomogeneities explicitly in time compromises the stability of the numerical scheme. Specifically, the explicit terms in (3.17) require $v\Delta t \max(\tilde{\sigma}_t) < 1$ for stability. This range is not restrictive in most applications since only a portion of the variable cross-sections is treated explicitly. However, if this stability condition does become problematic, an implicit fractional step method similar to that presented in [14] may be applied. Another possibility is to decompose the medium into strips over which the variable cross-sections are assumed to be piecewise constant with some variable perturbation. Then, one can construct and solve the corresponding layered background medium problem with the same method for inhomogeneous media presented above in each layer. This approach would minimize the size of the variable perturbation within each strip, thereby reducing the time step restriction.

3.3. Vector radiative transfer. Modifying the methods presented in section 2 to include polarization is straightforward. In fact, the only modification required lies

in constructing the system of equations for

$$\begin{bmatrix} I(s,\mu,t) \\ Q(s,\mu,t) \\ U(s,\mu,t) \\ V(s,\mu,t) \end{bmatrix} \cong \sum_{k=0}^{N} \begin{bmatrix} a_k^{(I)}(\mu,t) \\ a_k^{(Q)}(\mu,t) \\ a_k^{(U)}(\mu,t) \\ a_k^{(V)}(\mu,t) \end{bmatrix} T_k(s), \tag{3.19}$$

where $a_k^{(I)}$, $a_k^{(Q)}$, $a_k^{(U)}$, and $a_k^{(V)}$ are the spatial projections of the Stokes parameters onto the Chebyshev polynomial of order k. Proceeding in a similar manner as in section 2, we obtain

$$\frac{\partial}{\partial t} \begin{bmatrix} \mathbf{a}_k^{(I)} \\ \mathbf{a}_k^{(Q)} \\ \mathbf{a}_k^{(U)} \\ \mathbf{a}_k^{(V)} \end{bmatrix} + \frac{2v}{}$$

with

$$\mathcal{Q}[I] = \sigma_t I(s,x,\mu,\phi,t) - \sigma_s \int_0^{2\pi}\int_{-1}^{1} P(\mu,\mu',\phi-\phi')\, I(s,x,\mu',\phi',t)\, d\mu' d\phi'. \tag{3.26}$$

Boundary and initial conditions are given by (2.5b)–(2.5d) for all points x. Due to the $\cos\phi$ in front of the partial derivative with respect to x, the Fourier modes of the azimuthal variable do not decouple as in the one-dimensional problem. Therefore, the discrete ordinate method must be extended to include a quadrature rule for the azimuthal variable as well.

Since the medium is infinite in the horizontal direction, it is natural to deal with the x dependence of the intensity I by a Fourier series. Consequently, we approximate I by the expansion

$$I(s,x,\widehat{\Omega},t) \cong \sum_{k=0}^{N_v}\sum_{l=-N_h/2}^{N_h/2} a_{kl}(\widehat{\Omega},t) T_k(s) e^{ilx}. \tag{3.27}$$

Proceeding in an analogous way to section 2 we obtain a semidiscrete equation for each mode l that is decoupled from the others. Each decoupled semidiscrete equation has the same form as (2.15), where the operator $\mathcal{Q}$ has to be replaced by

$$\begin{aligned}\mathcal{Q}_l[a_{kl}](\mu,\phi,t) = {}& \sigma_t\, a_{kl}(\mu,\phi,t) + il\sqrt{1-\mu^2}\cos\phi\, a_{kl}(\mu,\phi,t) \\ & - \sigma_s \int_0^{2\pi}\int_{-1}^{+1} P(\mu,\mu',\phi-\phi')\, a_{kl}(\mu',\phi',t)\, d\mu' d\phi'.\end{aligned} \tag{3.28}$$

This problem can be solved by the same procedure as the one-dimensional case for each mode l independently. It is also clear that the case where the coefficients σ_t and σ_s depend on the position can be treated with a semi-implicit method as in section 3.2.

As a second example, let us consider that the horizontal direction is bounded by two planes at $x = 0$ and $x = d_x$ so that we have the two extra boundary conditions

$$I(z, x=0, \widehat{\Omega}, t) = 0 \qquad \text{on} \qquad \Gamma_x, \tag{3.29}$$

$$I(z, x=d_x, \widehat{\Omega}, t) = 0 \qquad \text{on} \qquad \Gamma_x, \tag{3.30}$$

where Γ_x denotes the set of points $[0,d_z]\times\mathbb{S}^2\times[0,T]$ such that $\nu(x)\cdot\widehat{\Omega} < 0$. After the linear transformation $r = 2x/d_x - 1$, we approximate the intensity I and its derivatives by the expansions

$$\begin{aligned} I(s,r,\widehat{\Omega},t) &\cong \sum_{k=0}^{N_v}\sum_{l=0}^{N_h} a_{kl}(\widehat{\Omega},t) T_k(s) T_l(r), \\ \frac{\partial}{\partial s} I(s,r,\widehat{\Omega},t) &\cong \sum_{k=0}^{N_v}\sum_{l=0}^{N_h} A_{kl}(\widehat{\Omega},t) T_k(s) T_l(r), \\ \frac{\partial}{\partial r} I(s,r,\widehat{\Omega},t) &\cong \sum_{k=0}^{N_v}\sum_{l=0}^{N_h} B_{kl}(\widehat{\Omega},t) T_k(s) T_l(r). \end{aligned} \tag{3.31}$$

Again, proceeding in a similar fashion we obtain the semidiscrete set of equations

$$\frac{\partial a_{kl}}{\partial t} + \frac{2v}{d_z}\mu A_{kl} + \frac{2v}{d_x}\sqrt{1-\mu^2}\cos\phi B_{kl} + v\mathcal{Q}[a_{kl}] = vF_{kl} \tag{3.32}$$

for $k = 0, 1, \ldots, N_v$ and $l = 0, 1, \ldots, N_h$. After discretization in the angular variables μ and ϕ and the time variable t, and using relations

$$a_{kl} = \frac{1}{2k}\left[c_{k-1}A_{k-1,l} - A_{k+1,l}\right], \tag{3.33a}$$

$$a_{kl} = \frac{1}{2l}\left[c_{l-1}B_{k,l-1} - B_{k,l+1}\right], \tag{3.33b}$$

one could resolve the resulting system for the $2(N+1)+(N+1)^2$ variables a_{0l}, B_{kN_h}, and A_{kl} as in section 2. However, this procedure is cumbersome due to the recursion relation between B_{kl} and A_{kl}. Therefore, we solve the fully discretized equations arising from (3.32) with an alternating direction implicit or approximate factorization method. The two-step method (see Appendix B) is

$$\left[\mathbb{I} + \frac{v\Delta t}{4}\mathrm{Q}\right]\mathbf{a}^*_{kl} + \frac{v\Delta t}{d_z}\mathrm{L}_z\mathbf{A}^*_{kl} = \left[\mathbb{I} - \frac{v\Delta t}{4}\mathrm{Q}\right]\mathbf{a}^n_{kl} - \frac{v\Delta t}{d_z}\mathrm{L}_z\mathbf{A}^n_{kl} + \frac{v\Delta t}{2}\left[\mathbf{F}^{n+1}_{kl} + \mathbf{F}^n_{kl}\right],$$

$$\left[\mathbb{I} + \frac{v\Delta t}{4}\mathrm{Q}\right]\mathbf{a}^{n+1}_{kl} + \frac{v\Delta t}{d_x}\mathrm{L}_x\mathbf{B}^{n+1}_{kl} = \left[\mathbb{I} - \frac{v\Delta t}{4}\mathrm{Q}\right]\mathbf{a}^*_{kl} - \frac{v\Delta t}{d_x}\mathrm{L}_x\mathbf{B}^*_{kl} \tag{3.34}$$

for each k and each l. The matrices Q, L_z, and L_x in (3.34) are defined in Appendix B. Algorithm (3.34) again has the desired property of preserving the structure of the one-dimensional problem. For each fixed l, one needs only to solve two block tridiagonal systems. This method is second-order accurate and unconditionally stable.

4. Numerical examples. Here, we present computations for different radiative transfer problems. We also examine the convergence of these methods in space and time. The convergence of the discrete ordinate method is well established [21]. Kim and Ishimaru [15] demonstrated that the Chebyshev spectral method, in conjunction with the discrete ordinate method, is able to resolve highly anisotropic scattering for these problems.

As an example, we consider a normally incident pulsed plane wave entering the medium at $z = 0$ and solve for the incoherent or scattered intensity. Figures 4.1(a) and (b) show the numerical solutions to scalar and vector problems, respectively. In these examples and all that follow, we normalize spatial units by $\ell = 1/\sigma_t^{(0)}$ and time units by ℓ/v.

For the scalar problem (Figure 4.1(a)), we computed the magnitude of the backscattered flux

$$\mathcal{F}(t) = 2\pi\int_{-1}^{0} I(z=0,\mu,t)|\mu|d\mu \tag{4.1}$$

for three different media of thickness $d = 20$. The scattering and absorption cross-sections

$$\sigma_{s,a} = \sigma^{(0)}_{s,a} + \tilde{\sigma}_{s,a}(z)$$

all have $\sigma^{(0)}_s = 0.98$ and $\sigma^{(0)}_a = 0.02$, and

$$\tilde{\sigma}_{s,a}(z) = A_{s,a}\exp\left[\left(\frac{z - z_{s,a}}{w_{s,a}}\right)^2\right].$$

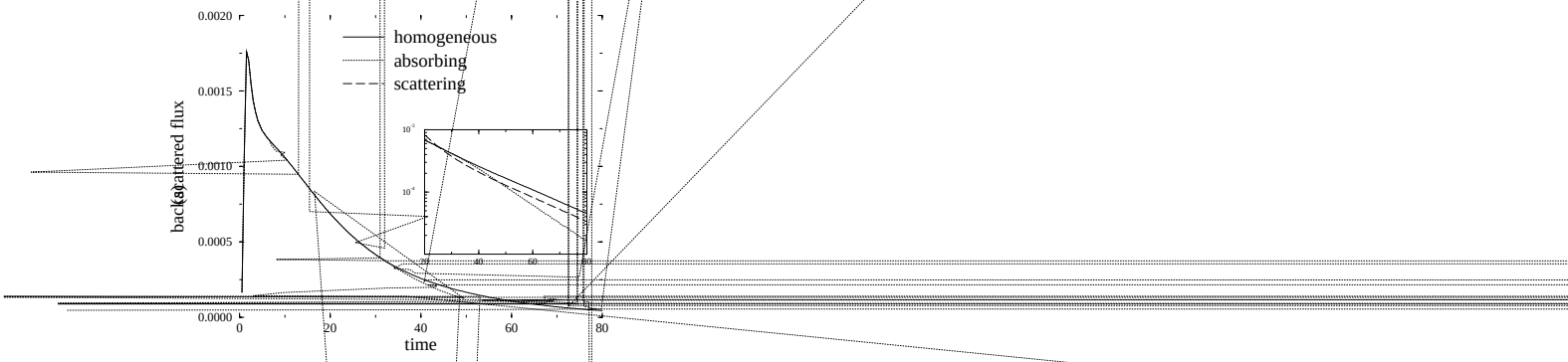
homogeneous
absorbing
scattering
backscattered flux
time
0.0020
0.0015
0.0010
0.0005
0.0000
0
20
40
60
80

Table 4.1
Parameter values for the three different media depicted in Figure 4.1(a).

Medium	A_s	z_s	w_s	A_a	z_a	w_a
homogeneous	0	—	—	0	—	—
absorbing	0	—	—	0.5	15	2
scattering	1	5	1	0	—	—

medium, thereby giving rise to the scattered component of the intensity [8]. The time at which the pulse center reaches the boundary at $z = 0$ is t_o and the pulse width is T. For this computation, $t_o = 1$, $T = 0.5$, and $g = 0.85$.

We observe in Figure 4.1(a) that the presence of the scattering inhomogeneity centered at $z_s = 5$ gives rise to an increase of the backscattered response (dashed line). By causality, the first indication of this presence takes place at $t \approx 11$. This is the time that it takes for light to propagate from the boundary to the inhomogeneity and back to the boundary. Similarly, we observe a decrease in the backscattered response at $t \approx 31$ due to the absorption inhomogeneity centered at $z_a = 15$ corresponding to the time needed to reach the inhomogeneity and return to the surface.

In Figure 4.1(b), we show the copolarized (solid line) and cross-polarized (dot-dashed line) components of the transmitted average intensity

$$\mathcal{U}(t) = \frac{1}{2}\int_0^1 I(z = d, \mu, t)d\mu.$$

The incident pulse is left-handed circularly polarized so that $I = V = 1$ and $Q = U = 0$ and normally impinges a medium of thickness $d = 1$. For these computations, $t_o = 1$ and $T = 0.5$. We define the copolarized intensity to be the component that is left-handed circularly polarized

$$I_{\text{LHC}} = \frac{1}{2}(I + V)$$

and the cross-polarized intensity to be the component that is right-handed circularly polarized

$$I_{\text{RHC}} = \frac{1}{2}(I - V).$$

Because early transmitted responses consist of light that has undergone very little scattering as it propagated through the medium, it is entirely copolarized. As time increases, scattering gives rise to depolarization so that the cross-polarized component increases. For very large times, we observe in Figure 4.1(b) that both components are equal.

4.1. Temporal convergence. To verify that the temporal discretization is second-order accurate, we examine time-resolved, backscattered flux responses for the scalar problems explained in sections 2, 3.1, and 3.2. As a test problem, we considered a pulse with $t_o = 1$ and $T = 0.5$ in a medium with thickness $d = 1$ and anisotropy $g = 0.5$ up to time $t = 10$. Since there is no known analytical solution to this problem, we compared flux responses using different time steps to a reference solution computed with $\Delta t = 0.001$. Specifically, we computed the infinity norm of the difference of a solution with lower resolution and the reference solution normalized by the infinity norm of the reference solution. For all of these computations, we used 20 quadrature points.

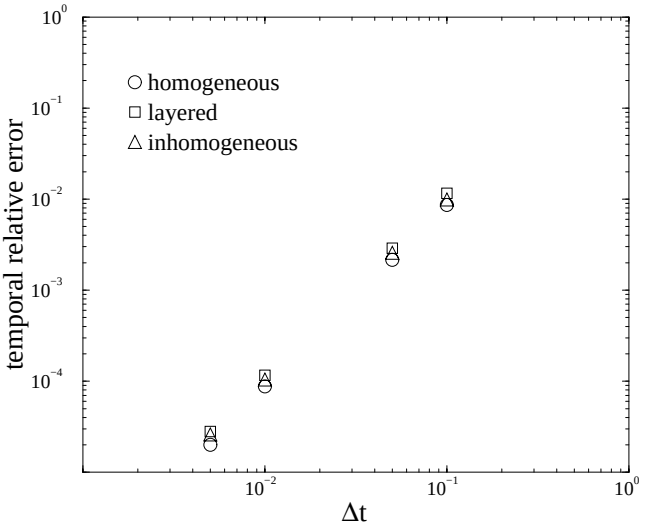

Fig. 4.2. *Computed relative errors of time-resolved, backscattered flux responses as a function of the time step Δt. These computations used 20 quadrature points. The medium is $d = 1$ thick with anisotropy $g = 0.5$.*

Table 4.2

Observed rates of convergence for the time discretization using the infinity norm of the difference between the computed solution and a reference solution with $\Delta t = 0.001$.

Medium	Convergence rate
homogeneous	2.0174
layered	2.0055
inhomogeneous	1.9874

For the homogeneous problem, we considered a medium with $\sigma_s = 0.98$ and $\sigma_a = 0.02$, and used 65 Chebyshev modes. For the layered problem, we considered three layers with interfaces at $z = 0.4$ and $z = 0.7$ with

$$\sigma_s(z) = \begin{cases} 0.98 & \text{for } z \in [0, 0.4], \\ 1.96 & \text{for } z \in (0.4, 0.7], \\ 0.90 & \text{for } z \in (0.7, 1], \end{cases} \qquad \sigma_a(z) = \begin{cases} 0.02 & \text{for } z \in [0, 0.4], \\ 0.04 & \text{for } z \in (0.4, 0.7], \\ 0.10 & \text{for } z \in (0.7, 1], \end{cases}$$

and used 17 Chebyshev modes in each layer. For the inhomogeneous problem, we considered

$$\tilde{\sigma}_s(z) = 0.98 \exp\left[-\left(\frac{z - 0.4}{0.3}\right)^2\right], \qquad \tilde{\sigma}_a(z) = 0.02 \exp\left[-\left(\frac{z - 0.4}{0.3}\right)^2\right],$$

and used 65 Chebyshev modes.

Plots of the backscattered flux errors appear in Figure 4.2. We tabulated the observed rates of convergence in Table 4.2. As expected, the time discretization exhibits a second-order convergence rate.

4.2. Spatial convergence. Since we use a Chebyshev spectral method to approximate the spatial dependence of the intensity, we expect a superalgebraic convergence as the number of Chebyshev modes increases. To isolate the spatial properties

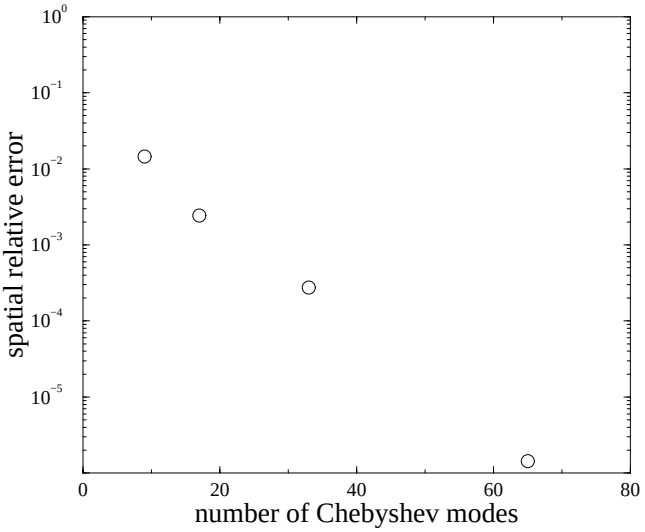

Fig. 4.3. *Relative errors of average intensities as a function of the number of Chebyshev modes for the continuous wave problem. These computations used* 60 *quadrature points for an isotropic medium* ($g = 0$).

of this method, we perform computations for a continuous wave source in a homogeneous medium with $\sigma_s = 0.98$ and $\sigma_a = 0.02$. Furthermore, we consider isotropic scattering ($g = 0$) with 100 quadrature points.

To model an incident continuous wave, we consider the limit in which the temporal pulse width tends toward infinity ($T \to \infty$). In that case, the source function is

$$F(z, \mu) = p(\mu, 1)\, \mathrm{e}^{-\sigma_t z}, \tag{4.6}$$

and, consequently, the specific intensity is independent of time.

To examine the convergence properties of the spatial approximation for this problem, we examine the average intensity

$$\mathcal{U}(z) = \frac{1}{2} \int_{-1}^{1} I(z, \mu) d\mu \tag{4.7}$$

computed using the Gaussian quadrature rule used with the scattering operator. As with the temporal convergence study, we do not have a known analytical solution. Instead, we compare results to a highly resolved reference solution with $N = 513$ Chebyshev modes.

A plot of this spatial convergence study appears in Figure 4.3. We compute the 2-norm of the difference between a particular solution and the reference solution normalized by the 2-norm of the reference solution. In Figure 4.3 we observe the expected superalgebraic convergence of this method. In fact, the relative errors for Chebyshev modes larger than 65 are below the allowed accuracy of double floating-point arithmetic.

5. Summary and concluding remarks. We have presented a complete discussion of Chebyshev spectral methods for solving radiative transfer problems. In particular, we have examined problems in which we apply Chebyshev spectral methods to the spatial variable, Gaussian quadrature methods to the angular variable, and

finite differences in the time variable. The resultant linear system of equations at each time step is sparse. This method easily handles homogeneous as well as continuously inhomogeneous and layered media. We have shown that these methods maintain the same structure and ease of implementation as the homogeneous problem. In addition, we show that it modifies easily to solve vector problems and has the potential to solve higher-dimensional problems efficiently.

For all of the cases presented here, we use the generalized deflated block elimination method to solve the bordered, block tridiagonal system of equations at each time step. This method is adequate in computing solutions for the problems we have examined here. However, it is noteworthy to mention that there is an obvious richness in the structure of this linear system beyond its sparsity (see Appendix A). It is quite possible that more can be done to take advantage of this structure to construct even more efficient methods for computing solutions. As we begin to implement this method for larger problems, examining this system in greater detail will become more important and hence will be the subject of future studies. Furthermore, we intend to use this method to examine polarization techniques for optical imaging problems in future work.

Appendix A. The generalized deflated block elimination method. To solve the system of equations (2.22) and (2.23) efficiently, let us construct two vectors that contain the unknown quantities,

$$X = \begin{bmatrix} \mathbf{A}_0, & \mathbf{A}_1, & \cdots, & \mathbf{A}_N \end{bmatrix}^T, \tag{A.1}$$

$$Y = \begin{bmatrix} \mathbf{a}_0 \end{bmatrix}, \tag{A.2}$$

where the superscript T denotes the transpose. Then, we can compactly write (2.22) and (2.23) as

$$\begin{bmatrix} A & B \\ C^T & D \end{bmatrix} \begin{bmatrix} X \\ Y \end{bmatrix} = \begin{bmatrix} F \\ G \end{bmatrix}. \tag{A.3}$$

Here, A is the $(N+1)\times(N+1)$ block tridiagonal matrix composed by $q \times q$ matrices M and K

$$A = \begin{bmatrix} \mathrm{M} & 0 & & & & & & & \\ \mathrm{K} & \mathrm{M} & -\frac{1}{2}\mathrm{K} & & & & & & \\ & \frac{1}{4}\mathrm{K} & \mathrm{M} & -\frac{1}{4}\mathrm{K} & & & & & \\ & & \ddots & \ddots & \ddots & & & & \\ & & & \frac{1}{2k}\mathrm{K} & \mathrm{M} & -\frac{1}{2k}\mathrm{K} & & & \\ & & & & \ddots & \ddots & \ddots & & \\ & & & & & \frac{1}{2(N-1)}\mathrm{K} & \mathrm{M} & -\frac{1}{2(N-1)}\mathrm{K} & \\ & & & & & & \frac{1}{2N}\mathrm{K} & \mathrm{M} & \end{bmatrix}, \tag{A.4}$$

B is the $(N+1)\times 1$ block column matrix

$$B = \begin{bmatrix} \mathrm{K}, & 0, & \ldots, & 0 \end{bmatrix}^T, \tag{A.5}$$

D is the $q \times q$ identity matrix, and C^T is the $1 \times (N+1)$ block row matrix

$$C^T = \begin{bmatrix} \mathbb{I}_0, & \frac{1}{4}\mathbb{I}_1, & \cdots, & \frac{1}{2}\left(\frac{1}{k+1} - \frac{1}{k-1}\right)\mathbb{I}_k, & \cdots, & -\frac{1}{2(N-1)}\mathbb{I}_N \end{bmatrix}, \tag{A.6}$$

where $\mathbb{I}_k$ is a $q \times q$ matrix made up of $\frac{1}{2}q \times \frac{1}{2}q$ submatrices

$$\mathbb{I}_k = \begin{bmatrix} \mathbb{I} & 0 \\ 0 & (-1)^{k+1}\mathbb{I} \end{bmatrix}. \tag{A.7}$$

The right-hand side vectors of this linear system are

$$F = \left[\mathbf{f}_0\,, \quad \mathbf{f}_1\,, \quad \cdots\,, \quad \mathbf{f}_N\right]^T, \tag{A.8}$$

$$G = \left[0\right]. \tag{A.9}$$

Each of the blocks in these matrices and vectors is $q \times q$. Therefore, (A.3) is a bordered, block tridiagonal system of equations.

By arranging the linear system of equations in this way, we can apply the generalized deflated block elimination method to solve this system [19]. This algorithm isolates the block tridiagonal part of this system from its borders, allowing one to exploit the sparsity. Contributions from the borders, B, C^T, and D come about as corrections to the block tridiagonal system solve. The generalized deflated block elimination algorithm is

1. solve $AW = B$,
2. solve $Aw = F$,
3. compute $S = D - C^T W$,
4. solve $SY = G - C^T w$,
5. compute $X = w - WY$.

In addition, the storage requirements in solving this system using this algorithm is very small. The diagonal blocks of A are diagonal matrices, and the off-diagonal blocks of A are all the same modulo a scalar factor. Therefore, only the $q \times q$ matrix, K, and a $q \times 1$ vector containing the diagonal elements of M are necessary to effectively store the matrix A. Furthermore, since each individual block in C^T are scalar multiples of identity matrices, computing the product of it and some other vector requires very few operations.

Appendix B. Alternating direction method. Replacing the continuous angular variables μ and ϕ by a set of discrete quadrature points μ_i and ϕ_j, where $i = 1, \ldots, q_1$ and $j = 1, \ldots, q_2$, we find that the semidiscrete spectral approximation (3.32) in matrix notation is

$$\frac{\partial \mathbf{a}_{kl}(t)}{\partial t} + \frac{2v}{d_z}\mathrm{L}_1\mathbf{A}_{kl}(t) + \frac{2v}{d_x}\mathrm{L}_2\mathbf{B}_{kl}(t) + v\mathrm{Q}[\mathbf{a}_{kl}](t) = v\mathbf{F}_{kl}(t) \quad \text{for } k, l = 0, \ldots, N, \tag{B.1}$$

with

$$\mathbf{a}_{kl}(t) = \left(a_{kl}(\mu_1, \phi_1, t), a_{kl}(\mu_1, \phi_2, t), \ldots, a_{kl}(\mu_1, \phi_q, t), \quad \ldots, \quad a_{kl}(\mu_{q_1}, \phi_{q_2}, t)\right), \tag{B.2}$$

and similar representations for $\mathbf{A}_{kl}$, $\mathbf{B}_{kl}$, and $\mathbf{F}_{kl}$. The $(q_1 q_2) \times (q_1 q_2)$ diagonal matrices L_1 and L_2 are defined by

$$\mathrm{L}_1 = \mathrm{diag}(\mu_1, \overset{q_2 times}{\cdots}, \mu_1, \mu_2, \overset{q_2 times}{\cdots}, \mu_2, \quad \ldots \quad \mu_{q_1}, \ldots, \mu_{q_1})$$

$$\mathrm{L}_2 = \mathrm{diag}(\mu_1 \cos\phi_1, \mu_1 \cos\phi_2, \ldots, \mu_1 \cos\phi_{q_2}, \quad \ldots \quad \mu_{q_1} \cos\phi_1, \ldots, \mu_{q_1} \cos\phi_{q_2}).$$

The Crank–Nicholson time-differencing scheme is given by

$$\text{(B.3)}\quad \left[\mathbb{I}+\frac{v\Delta t}{2}\mathrm{Q}\right]\mathbf{a}_{kl}^{n+1}+\mathrm{M}_1\mathbf{A}_{kl}^{n+1}+\mathrm{M}_2\mathbf{B}_{kl}^{n+1} = \left[\mathbb{I}-\frac{v\Delta t}{2}\mathrm{Q}\right]\mathbf{a}_{kl}^{n}-\mathrm{M}_1\mathbf{A}_{kl}^{n}-\mathrm{M}_2\mathbf{B}_{kl}^{n}+\frac{v\Delta t}{2}\left[\mathbf{F}_k^{n+1}+\mathbf{F}_k^{n}\right],$$

where $\mathrm{M}_1 = v\Delta t\mathrm{L}_1/d_z$ and $\mathrm{M}_2 = v\Delta t\mathrm{L}_2/d_x$. The expansion coefficients of the spatial derivatives B_{kl} and A_{kl} are related to a_{kl} through (3.33). Let us write formally the inverse relations of (3.33) as $A_{kl} = T_1 a_{kl}$ and $B_{kl} = T_2 a_{kl}$ so that we can make an approximate factorization of (B.3)

$$\text{(B.4)}\quad \left[\mathbb{I}+\frac{v\Delta t}{4}\mathrm{Q}+\mathrm{M}_1T_1\right]\left[\mathbb{I}+\frac{v\Delta t}{4}\mathrm{Q}+\mathrm{M}_2T_2\right]\mathbf{a}_{kl}^{n+1} = \left[\mathbb{I}-\frac{v\Delta t}{4}\mathrm{Q}-\mathrm{M}_1T_1\right]\left[\mathbb{I}-\frac{v\Delta t}{4}\mathrm{Q}-\mathrm{M}_2T_2\right]\mathbf{a}_{kl}^{n}+\frac{v\Delta t}{2}\left[\mathbf{F}_k^{n+1}+\mathbf{F}_k^{n}\right].$$

Observe that all the extra terms introduced in (B.4) are of order $O(\Delta t^2)$. Furthermore, the same terms are introduced in the left- and right-hand side. We can conclude that by subtraction of the extra terms in both sides of the equation, (B.4) is equivalent to (B.3) up to $O(\Delta t^3)$ (since $\mathbf{a}_{kl}^{n+1}-\mathbf{a}_{kl}^{n}\sim O(\Delta t)$). Then the two-stage method

$$\text{(B.5)}\quad \left[\mathbb{I}+\frac{v\Delta t}{4}\mathrm{Q}+\mathrm{M}_1T_1\right]\mathbf{a}_{kl}^{*} = \left[\mathbb{I}-\frac{v\Delta t}{4}\mathrm{Q}-\mathrm{M}_1T_1\right]\mathbf{a}_{kl}^{n}+\frac{v\Delta t}{2}\left[\mathbf{F}_k^{n+1}+\mathbf{F}_k^{n}\right],$$

$$\text{(B.6)}\quad \left[\mathbb{I}+\frac{v\Delta t}{4}\mathrm{Q}+\mathrm{M}_2T_2\right]\mathbf{a}_{kl}^{n+1} = \left[\mathbb{I}-\frac{v\Delta t}{4}\mathrm{Q}-\mathrm{M}_2T_2\right]\mathbf{a}_{kl}^{*}$$

solves (B.1). Again using that $A_{kl} = T_1 a_{kl}$ and $B_{kl} = T_2 a_{kl}$ we obtain the numerical scheme (3.34).

REFERENCES

[1] V. Borue and S. A. Orszag, *Self-similar decay of 3-dimensional homogeneous turbulence with hyperviscosity*, Phys. Rev. E, 51 (1995), pp. R856–R859.

[2] K. Black, *Spectral elements on infinite domains*, SIAM J. Sci. Comput., 19 (1998), pp. 1667–1681.

[3] M. D. Feit, J. A. Fleck, Jr., and A. Steiger, *Solution of the Schrödinger equation by a spectral method*, J. Comput. Phys., 47 (1982), pp. 412–433.

[4] R. Renaut and J. Frohlich, *A pseudospectral Chebyshev method for the 2D wave equation with domain stretching and absorbing boundary conditions*, J. Comput. Phys., 124 (1996), pp. 324–336.

[5] F. Ben Belgacem and M. Grundmann, *Approximation of the wave and electromagnetic diffusion equations by spectral methods*, SIAM J. Sci. Comput., 20 (1998), pp. 13–32.

[6] D. Gottlieb and S. A. Orszag, *Numerical Analysis of Spectral Methods: Theory and Applications*, SIAM, Philadelphia, 1977.

[7] C. Canuto, M. Y. Hussaini, A. Quarteroni, and T. A. Zhang, *Spectral Methods in Fluid Dynamics*, Springer-Verlag, Berlin, New York, 1988.

[8] A. Ishimaru, *Wave Propagation and Scattering in Random Media*, IEEE Press, New York, 1997.

[9] S. Chandrasekhar, *Radiative Transfer*, Dover, New York, 1960.

[10] L. Ryzhik, G. Papanicolaou, and J. B. Keller, *Transport equations for elastic and other waves in random media*, Wave Motion, 24 (1996), pp. 327–370.

[11] G. Bal and M. Moscoso, *Polarization effects of seismic waves on the basis of radiative transport theory*, Geophys. J. Int., 142 (2000), pp. 571–585.

[12] K. M. Case and P. F. Zweifel, *Linear Transport Theory*, Plenum Press, New York, 1967.
[13] M. Moscoso, J. B. Keller, and G. Papanicolaou, *Depolarization and blurring of optical images by biological tissues*, J. Opt. Soc. Amer. A, 18 (2001), pp. 948–960.
[14] B. Ritchie, P. G. Dykema, and D. Braddy, *Use of fast Fourier-transform computational methods in radiation transport*, Phys. Rev. E, 56 (1997), pp. 2217–2227.
[15] A. D. Kim and A. Ishimaru, *A Chebyshev spectral method for radiative transfer equations applied to electromagnetic wave propagation and scattering in discrete random media*, J. Comput. Phys., 152 (1999), pp. 264–280.
[16] O. Dorn, *A transport-backtransport method for optical tomography*, Inverse Problems, 14 (1998), pp. 1107–1130.
[17] L. M. Delves and J. L. Mohamed, *Computational Methods for Integral Equations*, Cambridge University Press, Cambridge, UK, 1985.
[18] E. A. Coutsias, T. Hagstrom, and D. Torres, *An efficient spectral method for ordinary differential equations with rational function coefficients*, Math. Comp., 65 (1996), pp. 611–635.
[19] T. F. Chan and D. C. Resasco, *Generalized deflated block-elimination*, SIAM J. Numer. Anal., 23 (1986), pp. 913–924.
[20] V. B. Kisslelev, L. Roberti, and G. Perona, *An application of the finite-element method to the solution of the radiative transfer equation*, J. Quant. Spectros. Radiat. Transfer, 51 (1994), pp. 603–614.
[21] H. B. Keller, *On the pointwise convergence of the discrete-ordinate method*, J. Soc. Indust. Appl. Math., 8 (1960), pp. 560–567.